Research Article
https://doi.org/10.33904/ejfe.1618187
© Copyright 2025 by Forest Engineering and Technologies Platform on-line at https://dergipark.org.tr/en/pub/ejfe

Eur J Forest Eng 2025, 11(2):95-105

EJFE

A Comparative Assessment of Sentinel-1 SAR with Optical Indices for Cloud-resilient Wildfire Mapping

Sohaib K. M. Abujayyab

Karabük University, Faculty of Humanities and Social Sciences, Department of Geography, 78050 Karabük, Türkiye

Abstract

Accurate and timely wildfire mapping is essential for effective post-fire management and mitigation. This study evaluates the potential of Sentinel-1 (S1) SAR VH cross-polarization data for burned area mapping in a Mediterranean forest ecosystem near Marmaris, Türkiye, and compares its performance with established optical indices from Sentinel-2 (S2) data. Post-fire imagery was analyzed using the NBR, NBRT1, and BAI indices, with accuracy assessed against Landsat 9 OLI data. The results showed that S2_NBR outperformed all other methods, achieving the highest overall accuracy (97.4%) and F1-score (0.97). S2_BAI and S2_NBRT1 also delivered strong results, while S1_SAR had a lower overall accuracy (69.2%) but achieved perfect precision (1), meaning it effectively avoided false positives. However, S1_SAR had limitations in detecting the full extent of burned areas (lower recall). SAR data, with its ability to penetrate clouds, highlights its value as a complement to optical methods by ensuring continuous monitoring when cloud-free optical imagery is unavailable. This study emphasizes the importance of combining data from multiple sensors for reliable wildfire monitoring and guide resource allocation, risk management, and recovery efforts.

Keywords: Wildfire mapping, Sentinel-1 SAR, NBR and NBRT1, BAI, Mediterranean ecosystem, Cloud-resilient.

1. Introduction

Wildfires play a major role in shaping ecosystems worldwide, affecting biodiversity, climate, and socio-economic conditions. In recent years, wildfires have become more frequent, intense, and widespread, making it even more critical to have effective ways to monitor and manage them (Sayad et al., 2019; ARSET, 2023; Zhang et al., 2024). Accurate and timely mapping of burned areas is essential for assessing damage, supporting recovery efforts, and improving predictions for future fire risks. Traditional methods like ground surveys, while reliable, are often slow, resource-intensive, and impractical for covering large areas. Satellite remote sensing has revolutionized wildfire monitoring by offering a wide-area view and enabling quick assessments of wildfire impacts (Zhang et al., 2024).

Optical remote sensing, using satellites like Sentinel-2, is particularly effective for mapping burned areas because it can detect changes in vegetation reflectance (Tanase et al., 2020; Pan et al., 2021; Saadat et al., 2022). Vegetation indices such as the Normalized Burn Ratio (NBR) and its differenced form (dNBR) use spectral data from near-infrared and shortwave infrared bands to measure burn severity (Gülci et al., 2021; Yüksel, 2022; A. Tariq et al., 2023). However, optical sensors face a key challenge: they depend on clear skies, and cloud cover often blocks the view, especially in fire-prone regions (Tanase, 2020). This limitation highlights the need to explore other options, such as weather-independent data sources, to ensure accurate and reliable burned area mapping (Sayad et al., 2019; Jain et al., 2020).

Synthetic Aperture Radar (SAR) systems, which operate in the microwave region of the electromagnetic spectrum, offer an effective way to overcome challenges caused by cloud cover. Unlike optical sensors, SAR sensors like Sentinel-1 send and receive their own signals, allowing them to capture data regardless of weather or sunlight. Studies have explored the use of Sentinel-1 for mapping burned areas, often combining its data with Sentinel-2 (De Luca et al., 2021, De Luca et al. 2022a, 2022b; A. Tariq et al., 2023). These studies have used methods like analyzing changes in backscatter, applying polarimetric decomposition techniques, and developing SAR-specific burn indices (De Luca et al., 2021). Combining SAR and optical data has shown great potential for improving accuracy, especially in complex landscapes (De Luca et al., 2022b). Optical imagery, such as Sentinel-2, provides high spatial and spectral

*Corresponding Author: Tel: +90 3704189660 E-mail: *sjayyab@karabuk.edu.tr*
Received: 14 January 2025; Accepted: 11 May 2025
This work is licensed under a Creative Commons Attribution-NonCommercial 4.0 International License

resolution, allowing for precise burned area mapping under clear-sky conditions. However, optical sensors are limited by cloud cover and smoke. SAR data, such as Sentinel-1, operates in the microwave spectrum and is unaffected by atmospheric conditions, enabling continuous monitoring of burned areas regardless of weather conditions. The integration of SAR and optical data enhances the reliability of wildfire detection, improves burn severity assessments, and increases the robustness of classification models by leveraging the strengths of both data types.

Research shows that SAR backscatter changes are linked to wildfire damage, such as changes in vegetation structure and moisture content. After a fire, vegetation loss and reduced moisture levels typically lead to lower backscatter, especially in cross-polarized channels like vertical-horizontal (VH) VH (A. Tariq et al., 2023). SAR polarimetry also provides valuable insights into how signals scatter in an area, helping to distinguish between burned and unburned vegetation (A. Tariq et al., 2023). While optical methods generally deliver higher accuracy for mapping burned areas approaches (Tanase et al., 2020), SAR's ability to work in all weather conditions makes it an important tool. This is especially true in regions with frequent cloud cover or during fast-changing fire events when timely data is critical.

This research focuses on assessing the potential of Sentinel-1 VH dual-band cross-polarization imagery for wildfire mapping. It examines how effective this data source is for detecting and outlining burned areas and explores its sensitivity to various burn severities and vegetation types. Taking advantage of SAR's cloud-resilient nature, the goal is to help create more reliable wildfire monitoring systems, especially in areas often affected by cloud cover.

2. Materials and Methods

2.1. Study Area

The study area is around Marmaris, a coastal town in Muğla Province, southwestern Türkiye. It covers a rectangular region with coordinates from 27.986471°E to 28.305156°E longitude and 36.779585°N to 36.957566°N latitude (Figure 1). Marmaris lies on the Mediterranean coast with a mix of mountains, valleys, and coastal plains. The area has a typical Eastern Mediterranean climate with hot, dry summers and mild, wet winters (Sari, 2021; S. Tariq et al., 2023).

Marmaris is prone to wildfires, especially in summer. While more specific historical fire data for the area may need to be sourced locally, Muğla Province has seen major fires in recent years (Baltaci and Yildirim, 2021). These fires have caused significant ecological and economic damage, highlighting the need for effective monitoring and management. The region's dry conditions, flammable vegetation, and challenging terrain make it prone to wildfires, with both natural vegetation and human settlements complicating firefighting efforts (Cigdem Cavdaroglu, 2021; Alkayiş et al., 2022; Tuna Tuygun et al., 2023).

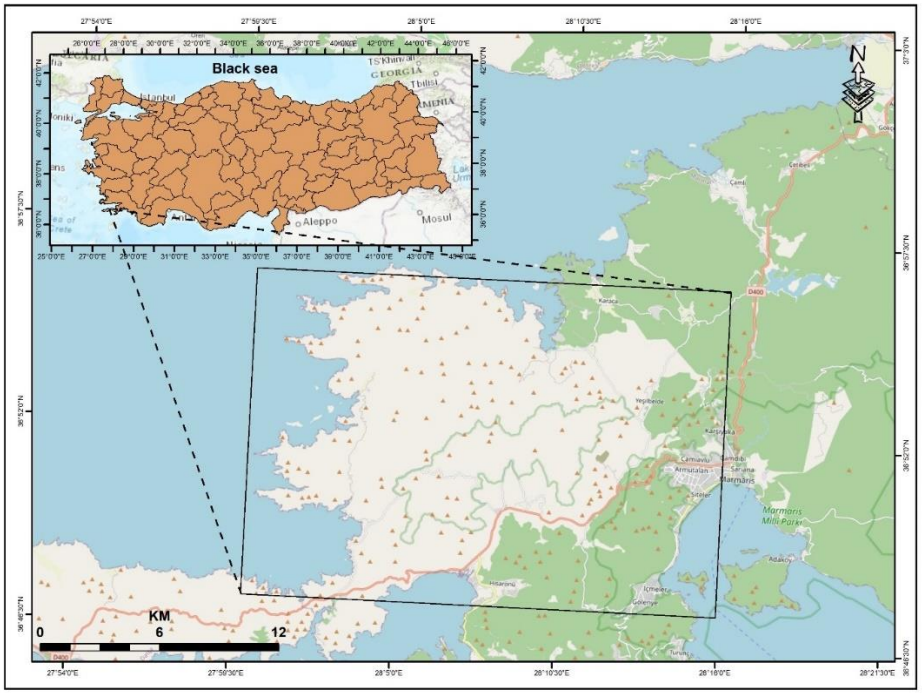


Figure 1. The location map of Study area, Marmaris, Türkiye

2.2. Data Acquisition and Preprocessing

This study uses Sentinel-1imagery for mapping burned areas in the Marmaris region. Data was collected before and after a wildfire event. The pre-fire period was from April 1, 2022, to June 10, 2022, and the post-fire period was from August 1, 2022, to August 15, 2022. Sentinel-1 data was acquired in Interferometric Wide swath (IW) mode, providing a good balance of coverage and resolution. VH polarization was chosen because it's sensitive to changes in vegetation structure after fires. Only ascending pass data was used to ensure consistency in imaging geometry.

In addition to Sentinel-1, Sentinel-2 optical imagery was also collected for the same pre- and post-fire periods (Figure 2.). Sentinel-2 data was mainly used for calculating burn indices and creating true-color (RGB) images of the study area. For accuracy assessment, a Landsat 9 Collection 2 Tier 1 surface reflectance product was used. Landsat 9 was launched on September 27, 2021, and provides multispectral imagery at a spatial resolution of 30 meters, a panchromatic band at 15 meters, and thermal imagery at 100 meters. It has 11 spectral bands, including Coastal/Aerosol, Blue, Green, Red, Near-Infrared (NIR), Shortwave Infrared (SWIR1 and SWIR2), Panchromatic, Cirrus, and two Thermal Infrared Sensor (TIRS1 and TIRS2) bands. Landsat 9 has a temporal resolution of 16 days, ensuring regular data acquisition for change detection and environmental monitoring. Images were captured between August 1 and August 28, 2022, during the post-fire period of Sentinel-1 data acquisition. The collection was filtered to include images with less than 10% cloud cover to ensure clear visibility of the area. This high-resolution Landsat 9 data was used as a reference for validating the burned area maps derived from Sentinel-1 and Sentinel-2.

2.3. Burned Area Mapping Methods

The proposed workflow for mapping wildfire burned areas combines Sentinel-1 SAR, Sentinel-2 optical data, and Landsat-9 as ground truth to create a cloud-resilient method. It starts with data preparation, which includes defining the study area, filtering datasets, and creating image mosaics. The next steps focus on preprocessing, with noise reduction applied to Sentinel-1 SAR imagery. Burned areas are identified using both optical and SAR thresholds through three indices from Sentinel-2: Normalized Burn Ratio (NBR), NBR Thermal 1 (NBRT1), and Burn Area Index (BAI). A fourth method based on Sentinel-1 SAR backscatter differences detects wildfire-related changes (S1_SAR).

Refinement steps, such as masking non-burned areas and filtering connected pixels, enhance the accuracy of the mapped burned regions. An accuracy assessment is performed using Landsat-9 data, and a comparative analysis highlights the benefits of the multi-sensor approach. This workflow leverages the strengths of both SAR and optical data, offering a scalable solution for wildfire monitoring in different environments.

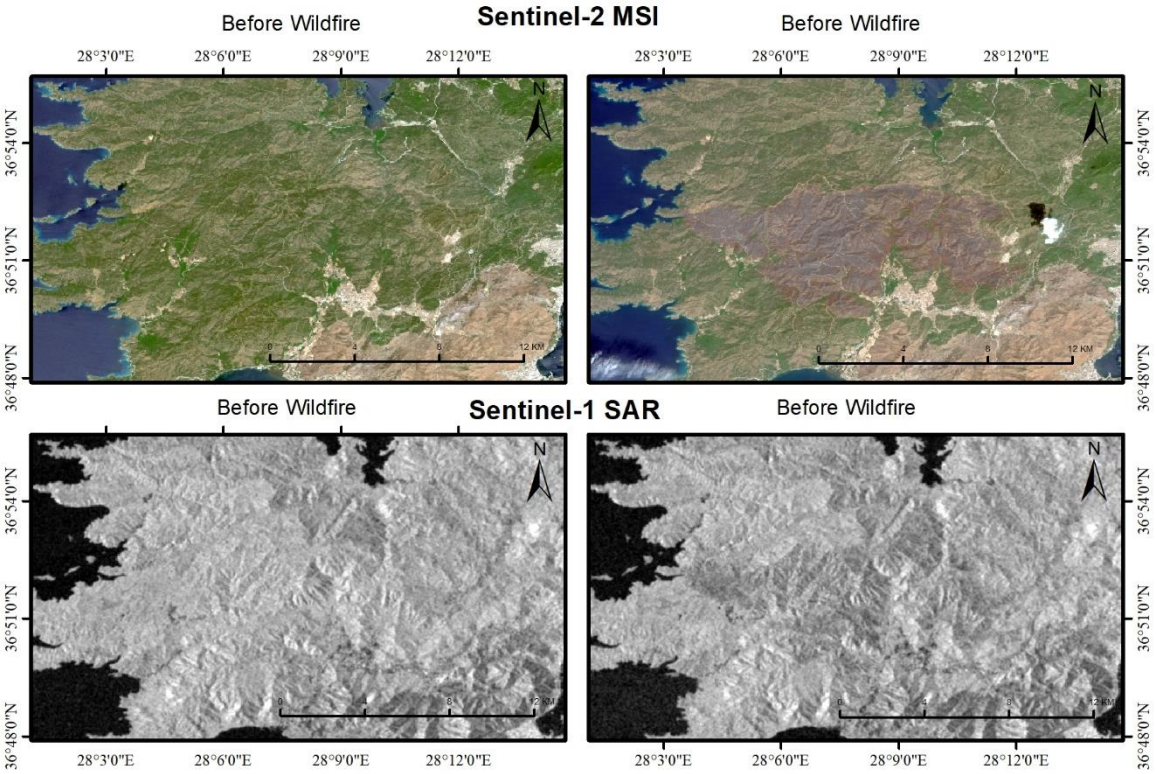


Figure 2. The original pre and post imagery of the Marmaris, Türkiye: (A) Sentinel-2 MSI image from June 8, 2022. (B) Sentinel-2 MSI image from August 10, 2022, showing burn scars. (C) Sentinel-1 SAR VH polarization image from June 10, 2022. (D) Sentinel-1 SAR VH polarization image from August 11, 2022.

2.3.1. Normalized Burn Ratio (NBR)

The Sentinel-2 NBR method uses the Normalized Burn Ratio (NBR), a spectral index sensitive to vegetation health, to assess burn severity. Sentinel-2 MSI data was collected for pre-fire and post-fire periods, focusing on Band 8A (near-infrared, NIR) and Band 12 (shortwave infrared, SWIR) (Ezzaher et al., 2024). Image collections for each period were filtered to the study area, and the NBR was calculated using the formula (Ezzaher et al., 2024):

$$\mathrm{NBR} = \frac{(\mathrm{NIR} - \mathrm{SWIR})}{(\mathrm{NIR} + \mathrm{SWIR})} \quad (1)$$

A median reduction was then applied to each collection to create representative composite images for the pre-fire and post-fire periods, minimizing the influence of outliers and atmospheric variability. The difference between post-fire and pre-fire NBR images (dNBR) was calculated to highlight areas where NBR decreased due to burning.

A threshold of -0.14 was applied to the dNBR image to generate a binary burned area mask. The ESA WorldCover map was used to exclude cropland, water, and built-up areas, minimizing false positives. A connected pixel filter with a threshold of 34 pixels was then applied to remove small, isolated patches of noise. This step enhanced the accuracy and spatial consistency of the final burned area map.

2.3.2. Normalized Burn Ratio Thermal 1 (NBRT1)

The Normalized Burn Ratio Thermal 1 (NBRT1) is a spectral index used to detect burned areas in satellite imagery by combining shortwave infrared (SWIR) and thermal infrared (TIR) bands. It enhances the traditional Normalized Burn Ratio (NBR) by adding thermal information, improving sensitivity to active fires and recent burns (Alcaras et al., 2022). NBRT1 is calculated using Sentinel-2 data by normalizing SWIR1 (Band 11) and SWIR2 (Band 12) reflectance values, dividing them by 1000, and applying the NBRT1 formula (Alcaras et al., 2022).

$$\text{NBRT1} = \frac{(\text{NIR} - (\text{SWIR} + \text{T1}))}{(\text{NIR} + (\text{SWIR} + \text{T1}))} \quad (2)$$

Median images for pre- and post-fire periods are computed to minimize atmospheric noise and cloud effects. A threshold value of -0.05 is applied to the NBRT1 difference image to identify burn areas effectively.

2.3.3. Burn Area Index (BAI)

The Burn Area Index (BAI) is another spectral index used to identify burned areas, relying on the reflectance characteristics of vegetation in the red and near-infrared (NIR) portions of the electromagnetic spectrum (Ezzaher et al., 2024). It quantifies the spectral difference between these bands and predefined values for burned areas, with the assumption that burned areas have distinctive spectral properties. Healthy vegetation typically exhibits high NIR reflectance and low red reflectance, while burned areas show the opposite pattern. The BAI is calculated as (Ezzaher et al., 2024):

$$\text{BAI} = \frac{1}{((0.1 - \text{Red})^2 + (0.06 - \text{NIR})^2)} \quad (3)$$

where RED and NIR represent the reflectance values of the red (Band 4) and NIR (Band 8A) bands, respectively. The resulting BAI values are then scaled by a factor of 10,000,000. The difference between the post-fire and pre-fire BAI images calculated to identify areas where BAI has significantly increased, indicating potential burns. A threshold (0.2) is applied to this difference image to classify pixels as burned or unburned.

2.3.4. SAR backscatter differences

The S1_SAR method uses changes in radar backscatter to detect burned areas, differing from optical indices. Its all-weather capability allows detection under cloud cover or at night. This approach focuses on changes in (VH) polarization, which reflects fire-induced alterations in vegetation structure and moisture content. Pre- and post-fire image collections were created, and mosaics were generated from individual Sentinel-1 tiles to cover the study area (Yoshioka et al., 2007; Pham-Duc et al., 2017; De Luca et al., 2021). To reduce speckle noise, a 50-meter focal mean filter was applied during preprocessing. The method's core involves calculating the ratio of post-fire to pre-fire backscatter. This ratio image highlights areas with significant changes caused by fire, computed for each pixel as:

$$\text{Backscatter Ratio} = \frac{(\text{Post} - \text{fire VH})}{(\text{Pre} - \text{fire VH})} \quad (4)$$

where:
- Post - fire VH is the VH polarization backscatter value from the post-fire image.
- Pre - fire VH is the VH polarization backscatter value from the pre-fire image.

A threshold was then applied to this ratio image to create a binary mask representing the burned area. Pixels with a ratio greater than the predefined threshold (1.15) were classified as burned:

$$Burned\ Area\ Mask = \begin{cases} 1, & \text{if Backscatter Ratio} > 1.15 \\ 0, & \text{otherwise} \end{cases}$$

2.4. Accuracy Assessment

In machine learning for imagery analysis, the following metrics are commonly used: overall accuracy, precision, recall, F1-score, specificity, AUC-ROC, and Cohen's kappa. These metrics provide a comprehensive evaluation of classification performance, balancing accuracy with false positive and false negative considerations.

The accuracy of the S1_SAR backscatter difference method was compared to three established burn area mapping methods: BAI, NBRT1, and NBR. Accuracy was evaluated using 500 ground truth points, evenly split between burned and unburned areas, based on a Landsat 9 reference image. This balanced sampling ensured an unbiased assessment of each method's performance. The evaluation used classified outputs from all four methods and their corresponding ground truth labels. A suite of performance metrics was calculated to comprehensively compare the methods. Metrics include standard metrics like true positives (TP), true negatives (TN), false positives (FP), and false negatives (FN), which serve as the foundation for calculating other crucial measures. These measures encompass overall accuracy (representing the proportion of correctly classified points); was calculated as:

$$\text{Overall Accuracy} = \frac{(TN + TP)}{(TN + TP + FP + FN)} * 100 \quad (5)$$

Misclassification rate, representing the proportion of incorrectly classified pixels, is the complement of accuracy. Precision, a measure of how many of the identified burned areas are truly burned, was calculated as:

$$\text{Precision} = \frac{TP}{(\text{TP} + \text{FP})} \quad (6)$$

Recall, quantifying the ability to correctly identify burned areas out of all actual burned areas, was calculated as:

$$\text{Recall} = \frac{TP}{(\text{TP} + \text{FN})} \quad (7)$$

The F1-score, providing a balanced measure of precision and recall, was calculated as:

$$\text{F1} - \text{score} = 2 * \frac{(\text{Precision} * \text{Recall})}{(\text{Precision} + \text{Recall})} \quad (8)$$

Specificity, measuring the ability to correctly identify unburned areas, was calculated as:

$$\text{Specificity} = \frac{\text{TN}}{(\text{TN} + \text{FP})} \quad (9)$$

The Area Under the Receiver Operating Characteristic Curve (AUC-ROC) assesses the discriminatory power of the method, representing the ability to distinguish between burned and unburned areas. Cohen's Kappa coefficient measures the agreement between the classified map and the ground truth, accounting for chance agreement. Cohen's kappa values range from -1 to 1. (1) indicates perfect agreement. (0) indicates no agreement other than what would be expected by chance. Negative values indicate less agreement than expected by chance. Cohen's Kappa coefficient was calculated as (Foody, 2020):

$$K = (\text{Po} - \text{Pe})/(1 - \text{Pe}) \quad (10)$$

where:

- Po, the observed agreement (the proportion of items on which the raters agree), was calculated as below:

$$\text{Po} = \frac{\sum_{i=1}^{k} n_{ii}}{N} \quad (11)$$

- Pe, the expected agreement (the proportion of agreement that is expected by chance), was calculated as below:

$$\text{Pe} = \frac{\sum_{i-1}^{k} (n_{i+} n_{+i})}{N^2} \quad (12)$$

Then, Kappa coefficient was found using following formula:

$$K = \frac{N \sum_{i=1}^{k} n_{ii} - \sum_{i-1}^{k} (n_{i+} n_{+i})}{N^2 - \sum_{i-1}^{k} (n_{i+} n_{+i})} \quad (13)$$

where;

n_{ii} : Number of samples correctly classified for class i, (burned areas correctly identified by both the classifier and reference data).

n_{i+} : Total samples classified into class i by the classifier (all areas classified as burned).

n_{+i} : Total samples labeled as class i in the reference data (burned areas in the ground truth dataset).

N : the total number of samples,

k : the number of classes (Burned and Unburned).

3. Results

3.1. Burned Area Results

Effective wildfire mapping requires methods that work under challenging conditions, including cloud cover and smoke. This study evaluates spectral indices and Sentinel-1 SAR VH cross-polarization imagery for detecting and mapping burned areas. Figure 3 compares these approaches, showing pre-fire and post-fire conditions alongside burned area maps. The rows represent NBRT1, NBR, BAI, and Sentinel-1 VH data, while the columns highlight temporal changes and burned areas visualized in red.

Spectral indices like NBRT1, NBR, and BAI effectively detect fire-induced vegetation loss. Pre-fire NBRT1 and NBR values indicate healthy vegetation, while post-fire values drop due to vegetation removal. Burned area maps from dNBRT1 and dNBR clearly delineate fire zones, making them suitable for large-scale mapping. BAI also captures burned areas well, with its ability to detect minor changes enhancing early fire detection, though it is less comprehensive for larger fire zones compared to NBR-based indices. Sentinel-1 SAR VH data complements optical methods by detecting structural changes in surface roughness. Pre-fire VH backscatter is high in vegetated areas, dropping significantly after fires due to vegetation loss. The resulting dVH map accurately identifies burned areas, particularly in cloudy or smoky conditions. Although SAR lacks the spatial detail of optical data, its cloud resilience ensures consistent monitoring. Combining optical and SAR data creates robust, all-weather wildfire mapping tools, offering valuable insights for fire management and recovery planning.

Figure 4 provides a comprehensive comparison of burn detection methods using Sentinel-1 SAR, Sentinel-2 MSI, and Landsat 9 OLI data. It highlights the strengths and limitations of each approach in mapping burned areas. The first row shows a Landsat 9 image as reference data, followed by rows illustrating burned area maps from Sentinel-2 indices (NBRT1, NBR, and BAI) and Sentinel-1 SAR VH data. Burned areas are highlighted in red, emphasizing the spatial extent of fire impacts.

The analysis shows clear differences in performance. Sentinel-2 indices (NBRT1, NBR, and BAI) demonstrate high accuracy, capturing burned areas with significant detail. NBRT1 and NBR are particularly effective, leveraging near-infrared and shortwave infrared sensitivity to vegetation loss and burn severity. BAI, while slightly less detailed, effectively captures broader burn patterns. Sentinel-1 SAR VH data provides a complementary perspective by detecting structural changes in surface roughness caused by fire. Although SAR data offers lower spatial resolution compared to optical indices, it remains valuable for burned area mapping under cloudy or smoky conditions where optical data is limited.

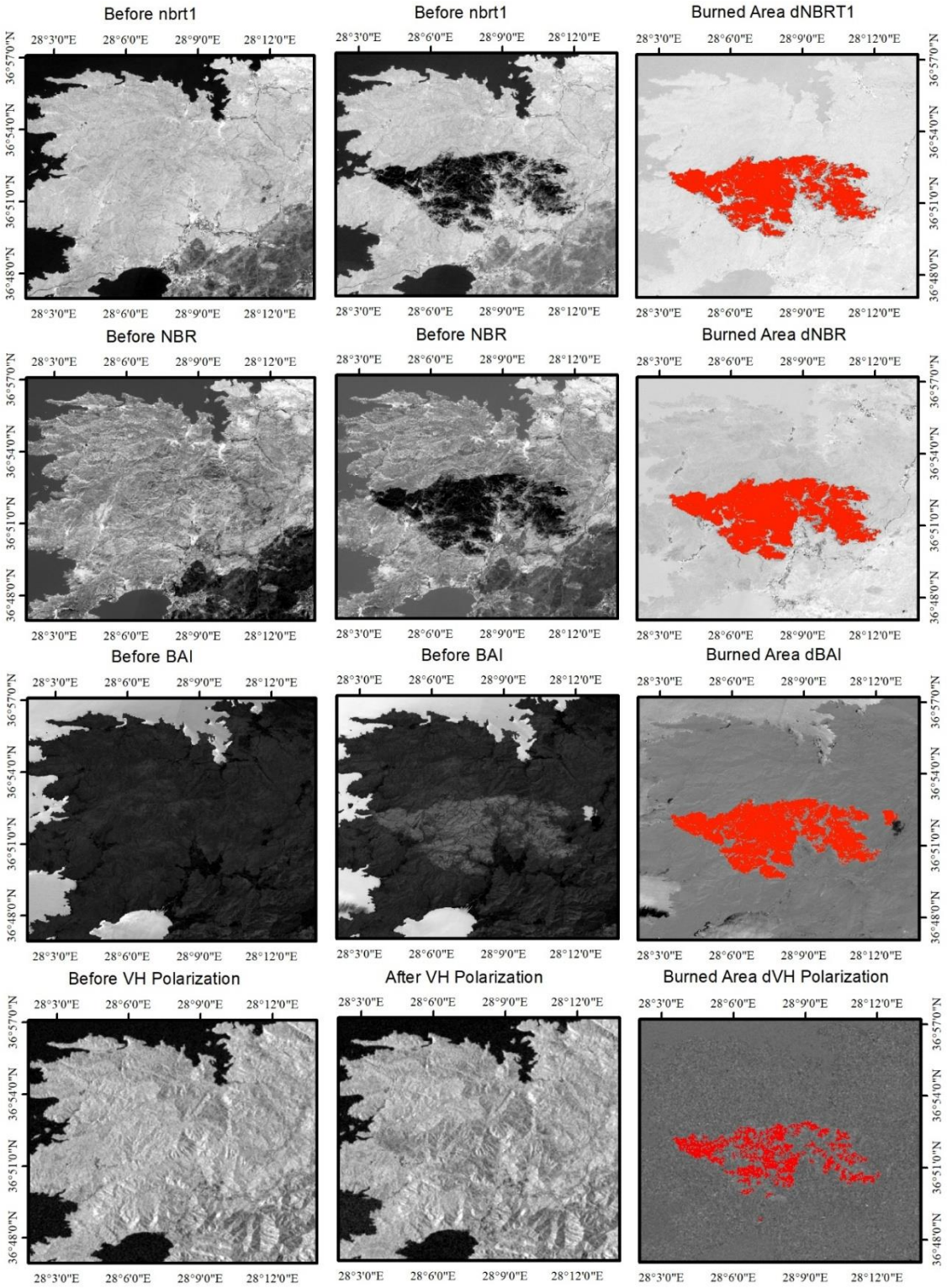


Figure 3. Mapping comparison of pre-fire conditions and after-fire conditions and spectral indices of burned areas using different methods (dNBRT1, NBR, and dBAI) and VH SAR polarizations for burned area detection

Burned area estimates varied across methods. Sentinel-2 indices mapped the largest areas, with S2_BAI identifying 40.2 km², followed by S2_NBR (39.6 km²) and S2_NBRT1 (34.3 km²). These differences reflect the indices varying sensitivity to vegetation loss and burn severity. In contrast, Sentinel-1 SAR VH data identified a smaller burned area of 16.3 km². While SAR maps lack the spatial detail of optical data, their ability to monitor under adverse conditions makes them essential for consistent wildfire mapping.

These findings underscore the advantages of integrating optical and radar-based methods for wildfire monitoring. Landsat 9 serves as a reliable reference, while Sentinel-2 indices provide detailed spatial mapping. Sentinel-1 SAR enhances robustness in challenging conditions. This multi-sensor approach improves the accuracy of burned area assessments and strengthens wildfire management strategies by addressing environmental and logistical constraints.

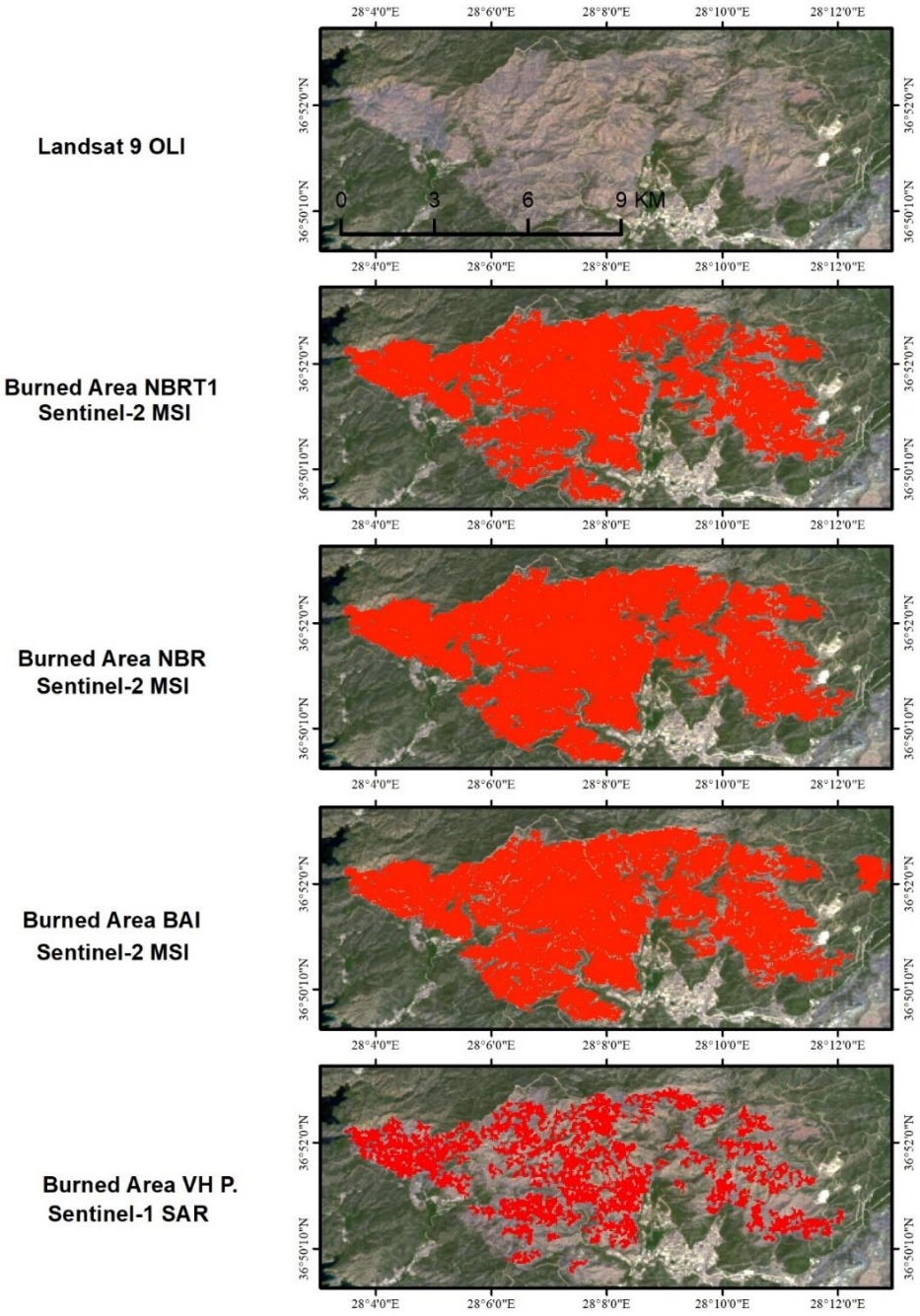


Figure 4. Comparison of burned area mapping techniques using Landsat 9 OLI, Sentinel-2 MSI (NBRT1, NBR, and BAI), and Sentinel-1 SAR VH polarization (The Landsat 9 OLI image serves as reference data)

3.2. Accuracy Assessment

Figure 4 summarizes the performance of four burned area mapping methods based on metrics derived from their respective confusion matrices. Key metrics such as true positives (TP), true negatives (TN), false positives (FP), false negatives (FN), overall accuracy, and misclassification rate are presented (Figure 5).

Among these methods, S2_NBR demonstrated the highest accuracy (97.4%) and the lowest misclassification rate (2.6%), followed by S2_BAI and S2_NBRT1. The S1 SAR approach exhibited the lowest accuracy (69.2%) and the highest misclassification rate (30.8%), highlighting substantial performance differences between optical and radar-based methods.

The analysis revealed that the S2_NBR method outperformed others, accurately classifying 97.4% of samples and showcasing its ability to capture fire-induced spectral changes. S2_BAI and S2_NBRT1 also demonstrated strong performance, with accuracies of 93.8% and 90.8%, respectively, though slightly less effective than S2_NBR. In contrast, the S1 SAR-based method struggled, with an accuracy of 69.2%, largely due to a high number of false negatives (FN = 154). This indicates challenges in detecting the full extent of burned areas using SAR data alone, despite its strength in avoiding false positives (FP = 0). The superior performance of S2_NBR and BAI highlights the effectiveness of optical indices for burned area mapping in this study, particularly in capturing spectral changes in near-infrared and shortwave infrared bands. These results emphasize the complementary nature of integrating optical and radar data for robust wildfire monitoring, especially under varying environmental conditions (Table 1).

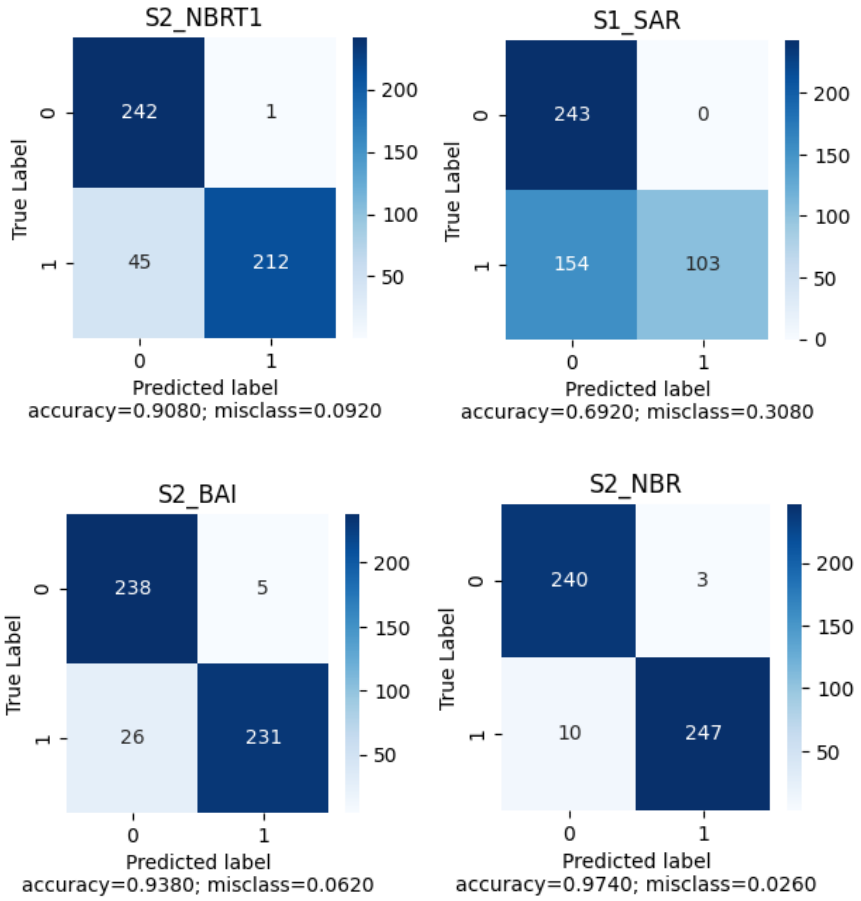


Figure 5. Confusion matrices for burned area detection using four methods: (a) S2 NBRT1, (b) S1 SAR, (c) S2 BAI, and (d) S2 NBR. Each matrix displays true positives, true negatives, false positives, false negatives, accuracy, and misclassification rate.

Table 1. Burned area detection performance metrics

Method	Overall Accuracy	Precision	Recall	F1 Score	Specificity	AUC-ROC	Kappa
S2_NBR	0.974	0.98	0.96	0.97	0.98	0.97	0.94
S2_NBRT1	0.908	0.99	0.82	0.90	0.99	0.91	0.81
S2_BAI	0.938	0.97	0.89	0.93	0.97	0.93	0.87
S1_SAR	0.692	1	0.40	0.57	1	0.70	0.39

Analysis of the performance metrics reveals distinct patterns in the efficacy of each burned area detection method. The S2_NBR demonstrates consistently high performance across all metrics, with a precision of 0.98, recall of 0.96, and a correspondingly high F1-score of 0.97. This indicates a strong balance between correctly identifying burned areas (high precision) and capturing the majority of actual burned pixels (high recall). The S2_BAI also performs well, achieving a precision of 0.97 and recall of 0.89, resulting in an F1-score of 0.93. While S2_NBRT1 exhibits the highest precision (0.99), its notably lower recall (0.82) impacts its overall F1-score (0.90), suggesting a tendency to miss some burned areas despite its high precision. The S1_SAR approach, while demonstrating perfect specificity (1) and consequently a perfect precision (1), suffers from a drastically lower recall (0.40), resulting in a significantly lower F1-score (0.57). This highlights the trade-off between minimizing false positives and capturing the true extent of the burned area; S1_SAR avoids misclassifying unburned areas as burned, but fails to identify a substantial portion of the actual burned areas. These trends are further corroborated by the AUC-ROC and Kappa values, with S2_NBR consistently outperforming other methods, followed by S2_BAI and then S2_NBRT1, while S1_SAR shows considerably lower performance. This suggests that optical-based methods, especially S2_NBR, are better suited for accurate and comprehensive burned area mapping in this context.

Evaluating the results reveals important insights into the strengths and limitations of each method for mapping burned areas under different conditions. Sentinel-2 spectral indices, NBR, NBRT1, and BAI, showed high sensitivity to fire-induced vegetation changes. Among these, NBR performed best, achieving 97.4% accuracy and an F1-score of 0.97, effectively capturing changes in vegetation reflectance in near-infrared and shortwave infrared bands. BAI and NBRT1 also performed well, with accuracies of 93.8% and 90.8%, respectively, though their sensitivity to burn severity and localized variations resulted in slight differences in mapped areas.

A key limitation of optical methods is their dependence on clear weather, as clouds and smoke can reduce data quality. Sentinel-1 SAR VH cross-polarization imagery addressed this issue by providing a weather-independent alternative. While SAR-based burned area maps were less detailed and accurate (69.2%) than optical methods, they effectively detected structural changes in vegetation and surface roughness, especially in cloudy conditions. SAR methods showed high precision (1), avoiding false positives, but their lower recall (0.40) and F1-score (0.57) indicate difficulty in fully capturing burned areas. This highlights the value of SAR for all-weather monitoring but also underscores the importance of combining SAR with optical methods for comprehensive wildfire mapping.

The analysis of burned area detection methods showed clear differences in accuracy and effectiveness. Optical indices consistently provided greater spatial detail and precision, making them essential for accurate wildfire mapping. In contrast, SAR data offered a valuable alternative, ensuring reliable monitoring in challenging conditions like cloud cover. Optical indices such as S2_NBR and S2_BAI proved highly effective for large-scale mapping and assessing burn severity, while SAR data ensured continuous monitoring when optical imagery was unavailable. Combining these methods addresses the challenges of wildfire monitoring, enabling timely and accurate assessments to guide resource allocation, risk management, and recovery efforts.

4. Discussion

The current study reports distinct performance metrics for burned area detection methods based on Sentinel-2-derived spectral indices namely S2NBR with an overall accuracy (OA) of 97.4%, S2NBRT1 with 90.8% OA, and S2BAI with 93.8% OA as well as for a Sentinel-1 SAR-based approach (S1SAR) with an OA of 69.2%.

Studies using optical imagery for burned area mapping have frequently reported overall accuracies exceeding 90%. For instance, Sobrino et al. (2024) demonstrated that the dNBR2 spectral index, derived from Sentinel-2 data, provided errors of 7% and 3% respectively, leading to high classification precision. In parallel, Wu introduced an optimized spectral index (ABAI) which reached an overall accuracy above 90%, indicating that optical methods can deliver robust detections (Wu et al., 2022). Farhadi reported an overall accuracy of 92.15% with a kappa coefficient of 0.92 for their burned area detection index based on Sentinel-2 imagery (Farhadi et al., 2023). In comparison, the S2_NBR method in this study achieves an OA of 97.4% with a kappa of 0.94, suggesting a significant improvement over several previously reported optical methods (Wu et al., 2022; Farhadi et al, 2023; Sobrino et al., 2024). While Yücer demonstrates high accuracy of optical indices (NDVI, NDMI, NBRI, BAI) derived from Sentinel-2 MSI and Landsat-9 OLI to assess burned areas (Yücer, 2023), this study asses Sentinel-1 SAR VH data with Sentinel-2 optical indices, thereby addressing limitations associated with cloud cover.

Conversely, the use of Sentinel-1 SAR data, particularly the VH polarization in the current study, results in a lower overall accuracy of 69.2%. This outcome is consistent with earlier investigations highlighting challenges in detecting burned areas using SAR imagery alone. Aguirre noted that while Sentinel-1 cross-polarization data is capable of detecting and quantifying burn scars, its sensitivity is generally lower compared to optical methods (Alarcon-Aguirre et al., 2022). Tariq reported an overall accuracy of approximately 82.3% for SAR-based burned area detection under dry conditions (Tariq et al., 2021). However, the lower recall observed (40%) in the current study's S1_SAR method points to limitations in capturing all affected pixels reliably, a limitation that has been documented in previous research where SAR data may miss small spectral changes in heterogeneous landscapes.

Furthermore, the S2NBRT1 method in this study, despite achieving a high precision (0.99), has a lower recall (0.82) and overall accuracy (90.8%), indicating a trade-off between the minimization of false positives and the detection of burned areas. This trade-off is similarly noted in other studies employing various spectral indices, where algorithm sensitivity to different fire severities and pixel heterogeneity impacts performance metrics. The optical indices specifically the S2NBR and S2_BAI approaches clearly outperform the SAR-based method, as evidenced by higher overall accuracies, F1 scores, and Kappa statistics, reinforcing previously observed patterns in burned area detection methodologies (Wu et al., 2022; Farhadi et al., 2023; Sobrino et al., 2024).

In summary, compared to earlier investigations, the high overall accuracy achieved by the Sentinel-2-based approaches in this research signifies a methodological advancement, potentially attributable to refined index calculations and post-processing techniques. In contrast, the reduced performance of the Sentinel-1 SAR method underscores the well-documented challenges associated with radar-based burned area detection, particularly in scenarios where minor vegetative and soil changes cannot be fully captured by SAR backscatter variations (Tariq et al., 2021; Alarcon-Aguirre et al., 2022).

5. Conclusion

This study highlights the value of integrating multi-sensor approaches for effective wildfire mapping. Sentinel-2 optical indices, especially the Normalized Burn Ratio (NBR), demonstrated exceptional accuracy (97.4%) in detecting fire-induced vegetation changes. The Burned Area Index (BAI) and Normalized Burn Ratio with Temperature 1 (NBRT1) also performed well, capturing detailed spatial patterns of burned areas. These results emphasize the strengths of optical data for wildfire mapping. Sentinel-1 SAR VH polarization data provided a reliable alternative in challenging conditions

like cloud cover or smoke. While less accurate spatially (69.2%) and with lower recall, SAR data effectively distinguished unburned areas and detected structural changes, making it valuable for consistent monitoring when optical data is unavailable. Combining optical and SAR data addresses the limitations of individual methods, enhancing the reliability of wildfire detection and mapping. Optical indices excel in burn Area's mapping but are limited by atmospheric conditions. SAR methods, though less detailed, ensure consistent monitoring in adverse environments. Future research should refine SAR-based techniques by exploring advanced backscatter modeling, coherence analysis, and integrating thermal data. Machine learning applied to multi-sensor datasets offers potential for improving accuracy and scalability.

Ethics Committee Approval: N/A.

Peer-review: Externally peer-reviewed.

Conflict of Interest: The authors have no conflicts of interest to declare.

Financial Disclosure: The author received no financial support for the research.

Cite this paper as: Abujayyab, S.K.M.2025. A Comparative Assessment of Sentinel-1 SAR with Optical Indices for Cloud-resilient Wildfire Mapping, *European Journal of Forest Engineering*, 11(2): 95-105.

References

Alarcon-Aguirre, G., Miranda Fidhel, R.F., Ramos Enciso, D., Canahuire-Robles, R., Rodriguez-Achata, L., Garate-Quispe, J. 2022. Burn Severity Assessment Using Sentinel-1 SAR in the Southeast Peruvian Amazon, a Case Study of Madre de Dios. *Fire*, 5(4): 94. https://doi.org/10.3390/fire5040094

Alcaras, E., Costantino, D., Guastaferro, F., Parente, C., Pepe, M. 2022. Normalized Burn Ratio Plus (NBR+): A New Index for Sentinel-2 Imagery. *Remote Sensing,* 14(7): 1727. https://doi.org/10.3390/rs14071727

Alkayiş, M.H., Karslioğlu, A., Onur, M.İ. 2022. Determination of forest fires risk potential map of Menteşe region of Muğla with geographic information systems, *Geomatik*, 7(1): 10–16.

ARSET, 2023. *Techniques for Wildfire Detection and Monitoring*. Available at: https://appliedsciences.nasa.gov/get-involved/training/english/arset-techniques-wildfire-detection-and-monitoring (Accessed: 4 September 2023).

Baltaci, U., Yildirim, F. 2021. Multi-criteria analysis and mapping of forest fire risk in Muğla Regional Directorate of Forestry, *Turkish Journal of Forestry Research*, 8(1): 1–11. https://doi.org/10.17568/ogmoad.708385.

Cigdem Cavdaroglu, G. 2021. Google Earth Engine Based Approach for Finding Fire Locations and Burned Areas in Muğla, Turkey, *American Journal of Remote Sensing*, 9(2): 72–77. https://doi.org/10.11648/j.ajrs.20210902.12.

Ezzaher, F.E., Ben Achhab, N., Raissouni, N., Naciri, H., Chahboun, A. 2024. Normalized Burn Ratio and Land Surface Temperature Pre- and Post-Mediterranean Forest Fires. *Environmental Sciences Proceedings*, 29(1): 3. https://doi.org/10.3390/ECRS2023-15829

Farhadi, H., Ebadi, H., Kiani, A. 2023. BADI: a novel burned area detection index for sentinel-2 imagery using google earth engine platform, *ISPRS Annals of the Photogrammetry, Remote Sensing and Spatial Information Sciences*, X-4/W1-2022, pp. 179–186. https://doi.org/10.5194/isprs-annals-X-4-W1-2022-179-2023.

Foody, G.M. 2020. Explaining the unsuitability of the kappa coefficient in the assessment and comparison of the accuracy of thematic maps obtained by image classification, *Remote Sensing of Environment*, 239: 111630. https://doi.org/https://doi.org/10.1016/j.rse.2019.111630.

Gülci, S., Yüksel, K., Gümüş, S., Wing, M. 2021. Mapping Wildfires Using Sentinel 2 MSI and Landsat 8 Imagery: Spatial Data Generation for Forestry. *European Journal of Forest Engineering,* 7(2): 57-66. https://doi.org/10.33904/ejfe.1031090

Jain, P., Coogan, S.C P., Subramanian, S.G., Crowley, M., Taylor, S., Flannigan, M.D. 2020. A review of machine learning applications in wildfire science and management. Environmental Reviews, 28(4): 478–505. https://www.jstor.org/stable/26998636

De Luca, G., M.N. Silva, J., Di Fazio, S., Modica, G. 2022a. Integrated use of Sentinel-1 and Sentinel-2 data and open-source machine learning algorithms for land cover mapping in a Mediterranean region, *European Journal of Remote Sensing*, 55(1): 52–70. https://doi.org/10.1080/22797254.2021.2018667.

De Luca, G., Silva, J.M.N., Modica, G. 2022b. Regional-scale burned area mapping in Mediterranean regions based on the multitemporal composite integration of Sentinel-1 and Sentinel-2 data, *GIScience and Remote Sensing*, 59(1): 1678–1705. Available at: https://doi.org/10.1080/15481603.2022.2128251.

De Luca, G., Silva, J.M.N., Modica, G. 2021. A workflow based on Sentinel-1 SAR data and open-source algorithms for unsupervised burned area detection in Mediterranean ecosystems, *GIScience and Remote Sensing*, 58(4): 516–541. https://doi.org/10.1080/15481603.2021.1907896.

Pan, L., Xia, H., Jia Wenhui N.Y., Wang, R., Song, H., Guo, Y., Qin, Y. 2021. Mapping cropping intensity in Huaihe basin using phenology algorithm, all Sentinel-2 and Landsat images in Google Earth Engine, *International Journal of Applied Earth Observation and Geoinformation*, 102(2021): 102376.

https://doi.org/https://doi.org/10.1016/j.jag.2021.102376.

Pham-Duc, B., Prigent, C., Aires, F. 2017. Surface water monitoring within cambodia and the Vietnamese Mekong Delta over a year, with Sentinel-1 SAR observations, *Water (Switzerland)*, 9(6): 366. https://doi.org/10.3390/w9060366.

Saadat, M., Seydi, S.T., Hasanlou, M., Homayouni, S. 2022. A Convolutional Neural Network Method for Rice Mapping Using Time-Series of Sentinel-1 and Sentinel-2 Imagery. Agriculture, 12(12): 2083. https://doi.org/10.3390/agriculture12122083

Sari, F. 2021. Forest fire susceptibility mapping via multi-criteria decision analysis techniques for Mugla, Turkey: A comparative analysis of VIKOR and TOPSIS, *Forest Ecology and Management*, 480(1): 118644. https://doi.org/10.1016/j.foreco.2020.118644.

Sayad, Y.O., Mousannif, H., Al Moatassime, H. 2019. Predictive modeling of wildfires: A new dataset and machine learning approach, *Fire Safety Journal*, 104: 130–146. https://doi.org/https://doi.org/10.1016/j.firesaf.2019.01.006.

Sobrino, J.A., Llorensa, R., Fernándezb, C., Fernández-Alonsob, J.M., Vegab, J.A. 2024. Methodology for Burned Areas Delimitation and Fire Severity Assessment Using Sentinel-2 Data. A Case Study of Forest Fires Occurred in Spain Between 2018 and 2023, *Recent Advances in Remote Sensing*, 5(27):1-13. https://doi.org/10.62880/rars240002.

Tanase, M.A., Belenguer-Plomer, M.A., Roteta, E., Bastarrika, A., Wheeler, J., Fernández-Carrillo, Á., Tansey, K., Wiedemann, W., Navratil, P., Lohberger, S., Siegert, F., Chuvieco, E. 2020. Burned Area Detection and Mapping: Intercomparison of Sentinel-1 and Sentinel-2 Based Algorithms over Tropical Africa. *Remote Sensing*, 12(2): 334. https://doi.org/10.3390/rs12020334

Tariq, A., Shu, H., Li, Q., Altan, O., Khan, M.R., Baqa, M.F., Lu, L. 2021. Quantitative Analysis of Forest Fires in Southeastern Australia Using SAR Data. *Remote Sensing,* 13(12): 2386. https://doi.org/10.3390/rs13122386

Tariq, A., Jiango, Y., Lu, L., Jamil, A., Al-ashkar, I., Kamran, M., Sabagh, A.E. 2023. Integrated use of Sentinel-1 and Sentinel-2 data and open-source machine learning algorithms for burnt and unburnt scars. *Geomatics, Natural Hazards and Risk*, 14(1). https://doi.org/10.1080/19475705.2023.2190856

Tariq, S., ul-Haq, Z., Mariam, A., Mehmood, U., Ahmed, W. 2023. Assessment of air quality during worst wildfires in Mugla and Antalya regions of Turkey, *Natural Hazards*, 115(2):1235–1254. https://doi.org/10.1007/s11069-022-05592-5.

Tuna Tuygun, G., İşsever, G., Elbir, T. 2023. Satellite Monitoring of Burned Forest Areas and Atmospheric Aerosols Originated from Major Forest Fires in Turkey in 2021. The Dokuz Eylul University Faculty of Engineering Journal of Science and Engineering, 25(74): 351-369. https://doi.org/10.21205/deufmd.2023257408

Wu, B., Zheng, H., Xu, Z., Wu, Z., Zhao, Y. 2022. Forest Burned Area Detection Using a Novel Spectral Index Based on Multi-Objective Optimization. *Forests*, 13(11): 1787. https://doi.org/10.3390/f13111787

Yoshioka, M., Fujinaka, T., Omatu, S. 2007. SAR image classification by support vector machine, Image Processing for Remote Sensing. CRC Press Boca Raton, FL, USA, pp. 624–637. https://doi.org/10.1201/9781420066654.ch15.

Yücer, E. 2023. Detection of Burned Areas with Sentinel-2 MSI and Landsat-9 OLI Satellite Images: 2022 Muğla/Marmaris Forest Fire, *Kahramanmaras Sutcu Imam University Journal of Engineering Sciences*, 26(4): 866–880. https://doi.org/10.17780/ksujes.1303299.

Yüksel, K. 2022. Evaluation of Different Remote Sensing Indices in Detection of Forest Burned Area: A Case Study of 2022 Mersin (Gülnar) Wildfire, *ArtGRID - Journal of Architecture Engineering and Fine Arts*, 4(2): 160–171. https://doi.org/10.57165/artgrid.1179074.

Zhang, P., Hu, X., Ban, Y., Nascetti, A., Gong, M. 2024. Assessing Sentinel-2, Sentinel-1, and ALOS-2 PALSAR-2 Data for Large-Scale Wildfire-Burned Area Mapping: Insights from the 2017–2019 Canada Wildfires. *Remote Sensing,* 16(3): 556. https://doi.org/10.3390/rs16030556